Available online at www.sciencedirect.com
SCIENCE DIRECT®
Carbon 43 (2005) 2600–2607
CARBON
www.elsevier.com/locate/carbon

Carbon membranes from cellulose and metal loaded cellulose

Jon Arvid Lie, May-Britt Hägg *

Department of Chemical Engineering, Norwegian University of Science and Technology, N-7491 Trondheim, Norway

Received 3 February 2005; accepted 12 May 2005
Available online 6 July 2005

Abstract

The focus of this work was to find a low-cost precursor for carbon molecular sieve (CMS) membranes, and a simple way of producing them. In addition, several ways of modifying a carbon material are described. The modification method used in this study was metal doping of carbon. CMS membranes were formed by vacuum carbonization of cellulose and metal loaded cellulose. Metal additives include oxides of Ca, Mg, Fe(III) and Si, and nitrates of Ag, Cu and Fe(III).

The carbon membrane containing Fe-nitrate has promising separation performance for the gas pairs O_2/N_2 and CO_2/CH_4. Carbon containing nitrates of Cu or Ag show high selectivity, but reduced O_2 and CO_2 permeability compared to carbon with Fe-nitrate. Element analysis indicates that Cu migrates to the carbon surface, creating an extra layer resistance to gas transport. A silver mirror is also seen on the surface of Ag-nitrate-containing carbon. However, the Ag- and Cu-containing membranes show a high H_2 permeability. Adding metal oxides makes the carbon membranes retard the transport of easily condensable gases (e.g. CO_2). This can be exploited for enhanced H_2/CO_2 separation efficiency.

Keywords: Molecular sieves; Carbonization, Doping; Scanning electron microscopy; Transport properties

1. Introduction

Two decades have passed since Koresh and Soffer [1] by simple thermochemical treatment produced molecular sieve carbon membranes for a continuous gas separation process. Since then, microporous carbon have been one of the most promising candidates for separation units in selected industrial gas streams, including upgrading of biogas to fuel quality and the application as CO_2 capture device in strategies for reducing global warming. In the petrochemical industry carbon membranes may comprise an efficient technique for separation of a paraffin from its corresponding olefin [2] and recovery of hydrogen from process streams.

Numerous possibilities exist for tailoring a carbon membrane for a specific separation. In the opinion of the authors, three main classes of modifications are recognized. Firstly, added compounds (hybride precursor matrix) that burn off during carbonization (temperature range 500–1000 °C), leaving a high micropore volume, may create high capacity membranes. Such additives may be referred to as porogens and can serve as templates in the formation of microporosity in carbon. The template size is likely to affect both the pore size distribution and the micropore volume (selectivity and permeability). An excellent example is siloxane units [–$Si(CH_3)_2$–O–] copolymerized with imide units [–$N(CO)_2$–C_6H_2–$(CO)_2$–N–R–] [3]: During carbonization most of the siloxane units burn off giving a high micropore volume, while the imide units are transformed to carbon rich domains with molecular sieving capability (high selectivity). Longer siloxane chains

* Corresponding author. Fax: +47 73594080.
E-mail address: may-britt.hagg@chemeng.ntnu.no (M.-B. Hägg).

0008-6223/$ - see front matter © 2005 Published by Elsevier Ltd.
doi:10.1016/j.carbon.2005.05.018

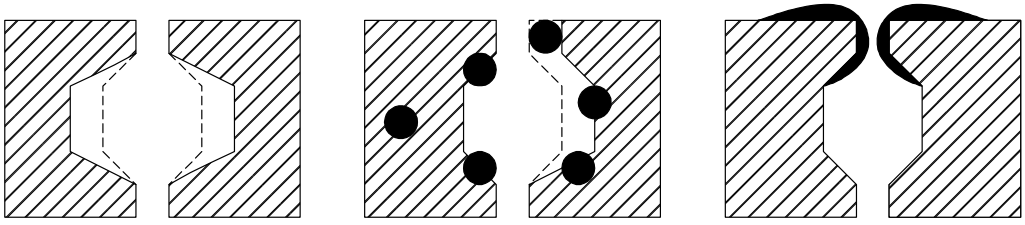

(a) Porogens (b) Doping/spacers (c) Surface modifiers

Fig. 1. Schematic model of different ways of tailoring microporous carbon. The dashed lines show the limit of an original, slit-shaped pore.

increase the gas permeability and reduce the selectivity of the C–SiO_2 membrane because of a more open membrane matrix. Another example of a porogen is polystyrene, used by e.g. Li et al. [4] in polycarbosilane, to increase the permeability. Post-oxidation of carbon also opens up the carbon structure by burning off e.g. alkyl side-chains, but at the same time oxygen-containing groups are introduced on the surface.

Secondly, mixing a carbon compatible thermally stable compound into the precursor (“doping”) may be suitable if interactions between the additive and the gas permeant can be exploited for an enhanced transport rate through the carbon membrane. One example is the formation of complexes between oxygen and silver [5]. Adding metals to the precursor may increase the micropore volume of the resulting carbon (a spacer effect) and cause electronic interactions, e.g. surface diffusion [6], with permeants like CO_2. If metals are added in the form of nitrates, the released NO_3^- from the carbonization may act as a porogen.

Thirdly, after carbonization the carbon surface may be modified by deposition of various compounds, including chemical vapor deposition (CVD), or by grafting of different molecules (e.g. chlorination or amination [7]). The three classes of modifications are depicted in Fig. 1. This article focuses on the first and second class, and presents the separation performance of cellulosic carbon, both in its pure form and when loaded with different metals.

The synthesis of a membrane should be cheap and simple in order to establish an economically viable separation unit. A cellulosic precursor was chosen in the current work. The cost of this precursor is as low as USD520/ADT (AirDried Ton),[1] and it is one of the most widespread and abundant biopolymers. Cellulose is a renewable and in-exhaustible resource.

Another demand is that the membrane should have a long-time stable flux (i.e. no significant aging), and sufficient mechanical strength to overcome fabrication as well as oscillating process conditions (pressure difference, temperature).

[1] For market prices, see www.foex.fi

The aim for the reported research has been to tailor a suitable, cheap carbon membrane for CO_2 recovery from various gas mixtures, with special focus on upgrading biogas to fuel quality.

2. Experimental

2.1. Materials

Wood pulp (also called kraft pulp) from a mixture of spruce and pine was supplied from Borregaard, Norway. It is composed of cellulose and hemicellulose in a ratio of 4 to 1.

Trifluoroacetic acid (TFA, 99%) and $Cu(NO_3)_2 \times 3H_2O$ (M_w 241.6) were supplied from Aldrich, Belgium. CaO, MgO, Fe_2O_3 and $AgNO_3$ were all supplied from Merck, Germany. SiO_2 was supplied from Elkem Thamshavn, Norway. $Fe(NO_3)_3 \times 9H_2O$ (M_w 404.1) was delivered from Fluka, Switzerland. Gases for permeation tests were supplied from AGA, Norway, with a purity of 99.9% or higher.

2.2. Film formation

The pulp was dissolved in TFA, to a concentration of about 1 wt.%. In the presence of TFA the 1,4-β-linkage is hydrolyzed with subsequent decrease in molecular weight. The TFA exposure time may have an effect on the separation performance, and this is under investigation. Exposure for about one week, i.e. one week from dissolving the cellulose in TFA until the film is dried under vacuum, resulted in inhomogeneous, non-selective carbon films. In the current work, the exposure time is 2–5 weeks for practical reasons.

A metal compound was then added in a concentration of 2–5% of the total precursor mass (solvent excluded). The metals used had two different forms: metal oxides (MeO) and metal nitrates (MeN). The metal oxides applied span a range of different adsorption enthalpies and electronegativities (as documented by Horiuchi et al. [6]). The metal ions also have different valences, a property that could be important for their interaction with the carbon matrix.

The solution was stirred overnight and then ultrasonicated with a VibraCell 130 (Sonics & Materials, Inc., CT, USA) 6 mm rod for 2 min at amplitude 80 μm. Unfortunately, the solutions containing CaO, MgO and Fe_2O_3 were not sonicated. However, when it comes to separation performance, it is shown later in this paper that the solubility of the MeO in TFA is more important than sonication of the solution. Then a film was cast on Teflon™ at room temperature. The film was covered to protect it from dust and to saturate the atmosphere above the film surface in order to slow down the evaporation rate, thereby increasing the homogeneity of the resulting film. Casting at 75 °C and 50 °C resulted in inhomogeneous films with bubble formations. The cast film precursor was left at room temperature and after 4 days finally dried in a vacuum oven at 105 °C for about 18 h.

2.3. Carbonization procedure

Films were carbonized under vacuum in a tubular furnace (Carbolite® TZF 12/100/900), using a working tube of alumina and a stainless steel grid as support for the films.

The protocol has a final temperature of 550 °C, kept for 2 h, a heating rate of 1 °C/min and several dwells. The protocol is pictured in Fig. 2, and is based on a protocol developed by Soffer et al. [8] for a cellulosic precursor. Their protocol was optimized with respect to mechanical properties of the carbon and its separation properties. The first two dwells are important in order to remove traces of water and solvent in the precursor. The other dwells are important in order to allow the carbon matrix to rearrange and form micropores in between turbostratically arranged layers of graphene sheets. In this work, the final temperature of 550 °C, kept for 2 h, was chosen because it was regarded as a moderate heat treatment. The main purpose was not to find the optimum carbon performance, but to identify trends in performance and obtain qualitative guidelines for material selection. After the final soak at 550 °C the system was allowed to cool naturally to a temperature less than 50 °C, before the furnace was purged with ambient air and the films removed.

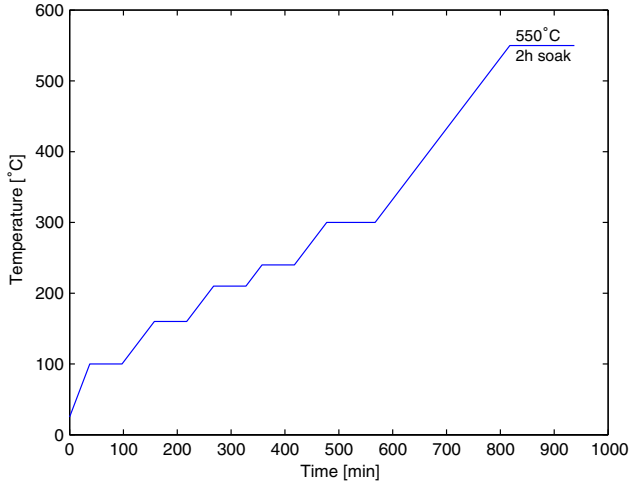

Fig. 2. Carbonization protocol (based on [8]).

2.4. Permeation tests

The carbon films were masked using an impermeable aluminum tape, leaving open a defined permeation area. Epoxy was then applied along the interface of the tape and the carbon. A sintered metal disc covered with a filter paper was used as support for the film in the test cell. Single gases were tested at 30 °C and a feed pressure of 2 bar (permeate side evacuated) in a standard pressure-rise setup (MKS Baratron® pressure transducer, 0–100 mbar range) with LabView® data logging. The experimental method and setup is described elsewhere [9,10]. The order of testing was always N_2, H_2, CH_4, O_2, CO_2, SF_6, and finally N_2 again to measure any degree of aging (productivity loss). This test order prevents the strongly adsorbing gases from disturbing the performance of the more ideal or non-interacting gases in carbon. The tests were run for several hours or days, to ensure that the transient phase of diffusion was passed. The permeation system was evacuated overnight in between each gas test.

2.5. Scanning electron microscope and element analysis

Scanning electron microscope (SEM) studies were performed on selected carbon films with a Hitachi S-3500N in the SE (secondary electron) mode. The samples studied had not been used in gas permeation tests, but were taken from the same carbonization batch as those used for permeation. All samples were stored in an exsiccator after carbonization, to minimize aging.

Element analysis (INCA software) was also carried out by measuring the K-line X-rays emitted from a selected area of the sample surface. Nickel was used as reference element.

3. Results and discussions

The composition of the precursor films are shown in Table 1, together with the weight loss during carbonization. The weight loss is consistent with results obtained by thermogravimetric analysis in nitrogen atmosphere (not shown here). Carbon yield may be increased by using a carbonization catalyst, e.g. HCl (g). In each carbonization batch, 6–8 smaller films (diameter typically 2.6 cm) from the same precursor were carbonized. In average, one third of the films produced could not be

Table 1
Composition of precursors and carbon films

Name of film	Metal source	MeO or MeN in precursor [wt.%]	Me in carbon film[b] [wt.%]	Carbonization weight loss [%]
C	–	–	–	81.1
C–CaO	CaO	4.9	15.5	76.8
C–MgO	MgO	4.9	9.9	69.3
C–FeO	Fe_2O_3	5.0	5.7	68.4
C–SiO	SiO_2	5.0	8.3	71.1
C–AgN	$AgNO_3$	3.8	11.2	78.4
C–CuN	$Cu(NO_3)_2$	4.0[a]	5.3	73.6
C–FeN	$Fe(NO_3)_3$	1.8[a]	1.4	69.0

[a] Crystal water subtracted.
[b] Theoretical value: assuming no loss of Me during carbonization.

tested, because they were too curved or wavy. All of the tested films gave reasonable results, indicating defect-free membranes.

The crystal water in the nitrates is assumed to dissolve in the TFA and evaporate during vacuum drying of the films.

The gas transport properties are summarized in Table 2. Numbers are single point values from single characterization experiments. The greatest contribution to uncertainty in the permeability values is believed to originate from variations in film thickness (±10%, Table 2), a result of gradients in the precursor film thickness. The carbon membrane without additives shows no aging after the gas test series, i.e. after about 7 days. In fact there is an increase in N_2 permeability, which may result from a flushing effect of H_2 or N_2. The same may be the case for the CaO film. In contrast, when adding the other metal oxides significant aging occurs. Especially MgO seems to be a strong adsorbent for O_2, CO_2 and SF_6.

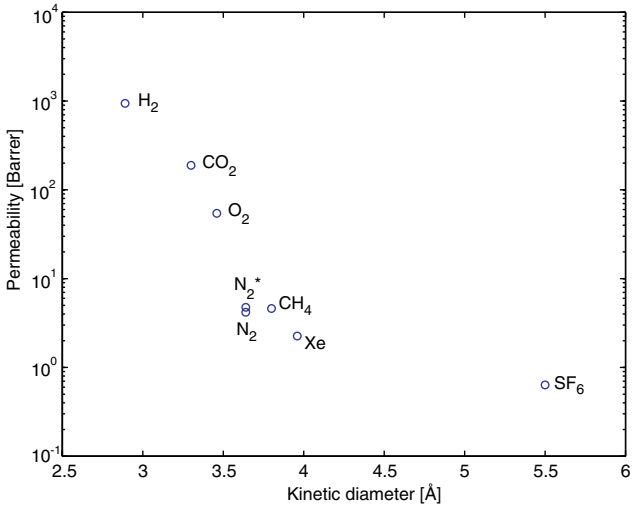

Fig. 3. A permeability vs. gas kinetic diameter plot of pulp carbonized at 550 °C for 2 h. Nitrogen was tested both as the first (N_2) and the last (N_2^*) gas in the series, to study aging of the membrane.

3.1. Pore size indication and aging of carbon without additives

The resulting membranes were characterized by making a plot of the permeability of the different probe gases as a function of their kinetic diameter as shown by Breck [11]. The plot for the carbon film without any metal loading is given in Fig. 3, and shows the sharpest cut at approximately 3.5 Å.

3.2. Thermal stability of metal compounds

Metal oxides (MeO) are known to be stable at high temperatures, whereas metal nitrates (MeN) probably

Table 2
Results from carbonization of wood pulp (2 bara at feed side, 30 °C)

Film	Thickness [micron] ± 2SD	P_{N_2} [Barrer]	P_{H_2} [Barrer]	P_{CH_4} [Barrer]	P_{O_2} [Barrer]	P_{CO_2} [Barrer]	P_{SF_6} [Barrer]	Aging [% change in N_2 permeability]
C	40 ± 4	4.2	9.4×10^2	4.6	54	1.9×10^2	0.63	+14
C–CaO	49 ± 4	3.1	8.6×10^2	3.5	38	1.3×10^2	4.8	+16
C–MgO	61 ± 3	4.4	11×10^2	1.2	5.5	14	0.37	−84
C–FeO	71 ± 9	8.3	2.8×10^2	4.0	30	1.1×10^2	2.0	−43
C–SiO	50 ± 6	1.9	6.7×10^2	2.0	19	58	0.66	−10
C–AgN	24 ± 3	5.1	15×10^2	1.4	53	1.8×10^2	0.55	−21
C–CuN	63 ± 4	2.3	11×10^2	0.66	25	81	0.24	−16
C–FeN	75 ± 8	8.2	10×10^2	2.1	86	3.1×10^2	0.64	−3

decompose to MeO and NO_x. CuN seems to form CuO with evaporation of the remaining nitrate groups, according to Silverstein et al. [12]. The following reaction may take place during carbonization:

$$Cu(NO_3)_2\ (s) \rightarrow CuO\ (s) + NO\ (g) + NO_2\ (g) + O_2\ (g) \quad (1)$$

A similar degradation is assumed for AgN and FeN. The release of gases should make the MeN-containing membranes more open-structured and permeable than the membranes with MeO added. The released gases may to a large extent contribute to the formation of micropores, in addition to the reduction and rearrangement of the cellulosic carbon itself. Thus the nitrates may be regarded as porogens (Fig. 1a).

But more important in this study is the reaction between TFA and the metal nitrates, forming MeTFAc (metal trifluoroacetate) and nitric acid:

$$TFA\ (aq) + MeN\ (s) \rightarrow MeTFAc\ (aq) + HNO_3\ (aq) \quad (2)$$

The TFAc helps distributing the metal in the solution and may act as a porogen in the carbonization of the films. Except for CaO, the MeOs are not easily dissolved in TFA at the temperature and concentration used in this work.

3.3. O_2/N_2 separation

The separation performance of the different membranes for O_2/N_2 separation is shown in Fig. 4, and compared to the trade-off line for polymers [13]. The permeability of the relevant gases in the precursor is not given here, because it was equal to or close to the leak rate of the permeation system. The very positive effect of carbonization is however clear; cellulose is transformed from a glassy, dense film to a highly microporous film with excellent selectivity and high permeability. When aging is considered, the carbon without any metal additive is the most promising material (Table 2). Except for the C–CaO film, the nitrate films seem superior to the oxide films. The FeN-film has a higher permeability than the carbon without any additive, whereas the other nitrate-containing films are at the same level or less permeable than the pure carbon. This only partially supports the idea that porogens are active. The high permeability of the FeN-film may be explained by the high number of nitrate groups, acting as porogens. In the case of AgN, it is possible that most of the Ag diffuses to the surface of the membrane, forming a silver mirror [14] and hence an additional resistance to mass transfer. By eyesight a large amount of silver can be observed on the carbon surface. This phenomenon was not verified in the case of CuN (see Section 3.7), but the reduced permeability, compared to pure carbon, suggests that Cu adds some resistance to the transport of oxygen.

The oxides seem to retard the oxygen transport. The reason why CaO gives the best performance among the oxides, is probably its good solubility in TFA, resulting in a homogeneous C–CaO matrix.

By adding metals, the selectivity of O_2/N_2 is slightly reduced.

3.4. CO_2/CH_4 separation

Two distinct groups of materials are visible from Fig. 5: oxides and nitrates. The performance of the nitrate-containing films may be explained in the same

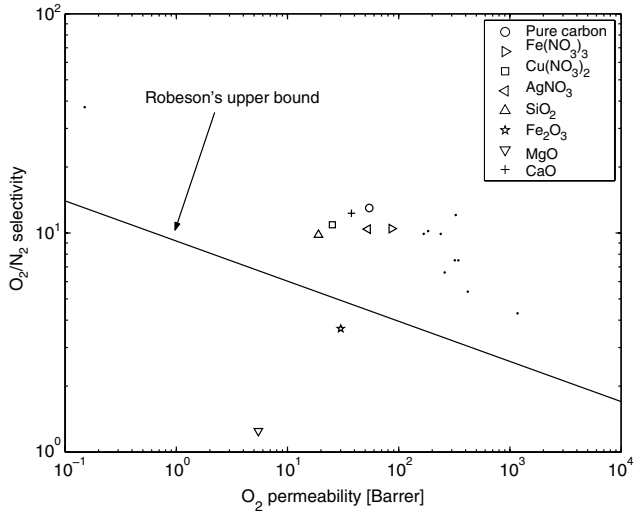

Fig. 4. Separation performance of carbon and metal loaded carbon for the O_2/N_2 gas pair at 30 °C. The N_2 value used is from the first N_2 test in the test series, and not from the repetition test. Dots are literature values for carbonized polyimides [3,15–18].

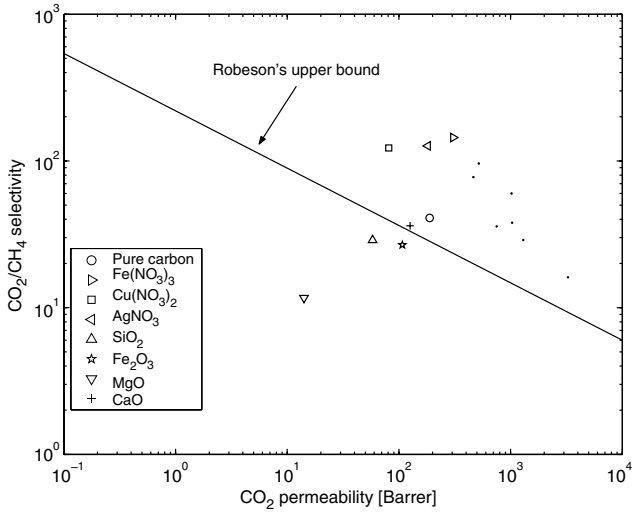

Fig. 5. Separation performance of carbon and metal loaded carbon for the CO_2/CH_4 gas pair at 30 °C. Dots are literature values for carbonized polyimides [15,17].

way as for the O_2/N_2 separation. The FeN-membrane has the highest amount of nitrate groups and is also the most CO_2-permeable membrane. Cu and Ag may form additional resistance. Addition of MeN also seems to block CH_4.

All the oxides retard the transport of CO_2, and are apparently more suitable as adsorbents for this gas than as membranes. Their performance is in the range of polymers, and not in the upper right corner of Fig. 5, which is the commercially attractive region.

3.5. H_2/CO_2 separation

Fig. 6 pictures the performance of the membranes with respect to H_2/CO_2 separation. This separation may for instance be used to increase the conversion of the water–gas shift reaction. The performance of the MgO-containing carbon is associated with some uncertainty because of a strong aging effect (Table 2).

3.6. H_2/CH_4 separation

Fig. 7 clearly shows that by adding metals, either as nitrate or oxide (except for iron oxide), a significant improvement is achieved. This is probably due to a combination of a spacer effect (increasing the hydrogen permeability) and a blocking of methane molecules. An increased content of metal, especially Ag and/or Cu, may facilitate the transport of hydrogen, since protons (H^+) can permeate through clusters of these metals as well (like in bulk metal membranes).

Fig. 7 gives useful guidelines if separation of hydrogen from natural gas is wanted, like in a system or society with a common infrastructure for hydrogen and natural gas. The performance of carbon membranes is superior to that of polymers. The polyimides perform better than cellulose.

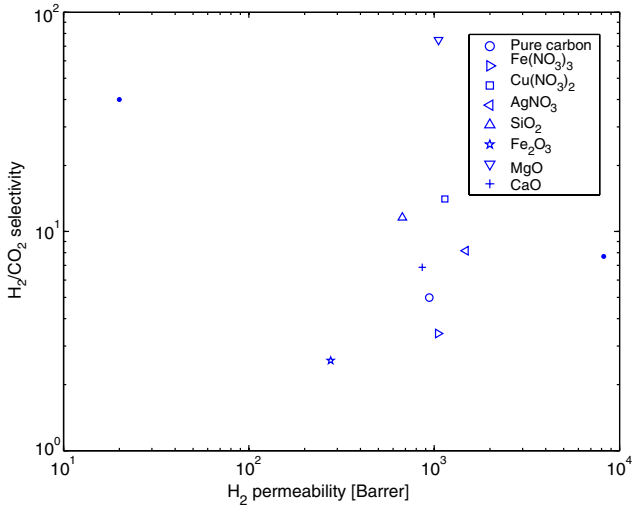

Fig. 6. Separation performance of carbon and metal loaded carbon for the H_2/CO_2 gas pair at 30 °C. Dots are literature values for carbonized polyimides [3,18].

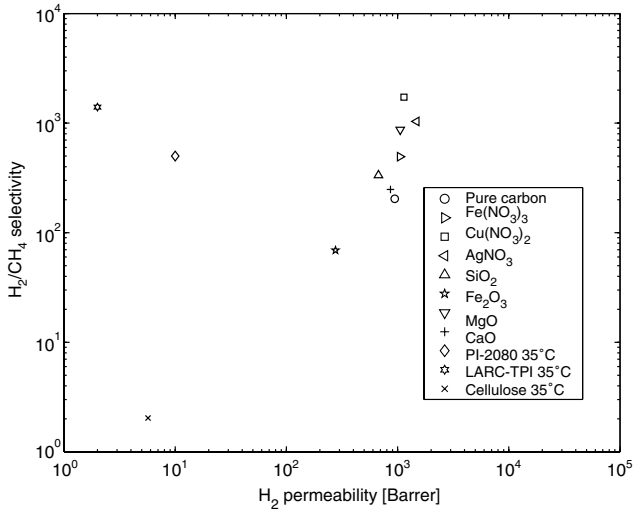

Fig. 7. Separation performance of carbon and metal loaded carbon for the H_2/CH_4 gas pair at 30 °C. Polyimides (PI-2080 and LARC-TPI) [19] and water-swollen cellulose [20] are included for comparison.

In summary, the separation performance of cellulosic carbon with metal additives is at the same level as carbons derived from specialty polymers like polyimides. The advantage of cellulose is its abundance and low cost. No catalyst is used during the carbonization, as opposed to procedures published by other research groups using cellulosic precursors (see e.g. [8]). This makes the membrane synthesis simpler, and economically more viable. On the other hand, the mechanical properties of a metal loaded cellulose carbon may not be as good as those of carbons from polyimides. The cellulose precursor films, both pure and metal loaded, are flexible immediately after vacuum drying at 105 °C, but become brittle after cooling to room temperature. In practice, e.g. for hollow fiber spinning, the metal should be more firmly bound in the precursor matrix to avoid dissolution of the metal in the bath or in the liquids used. This also provides a more uniform cross-section. Barsema et al. [21] managed to bind Ag^+ ionically in sulfonated poly(ether ether ketone).

3.7. SEM and element analysis

Fig. 8 shows a cross-section of the carbon membrane without any metal additive. No significant asymmetry can be deduced from the SEM picture, but a more coarse structure in the middle of the cross-section may be suspected. Nitrogen adsorption at 77 K (SA3100+, Beckman Coulter™, CA, USA) revealed a significant amount of meso- and macroporosity in these membranes. In the pure carbon film, 34% of the pores had a pore diameter less than 6 nm, while only 31% were smaller than 6 nm in the C–FeN.

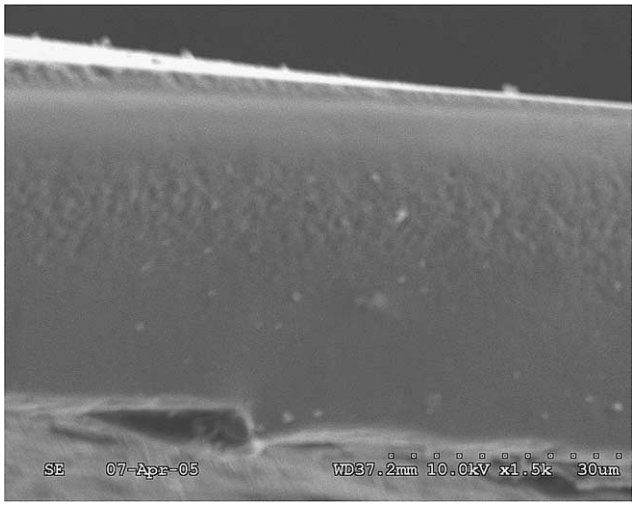

Fig. 8. SEM picture of the pure carbon membrane cross-section. Lower part pictures the surface underneath the film.

SEM pictures of the surface of the C–CuN membrane were taken (not shown). The particles were difficult to see in the microscope and therefore assumed to be well distributed. This supports the theory that the solvent TFA reacts with and distributes the metal nitrates. In contrast, on the SEM picture of a C–FeO film (Fig. 9), large particles (up to 10 μm) can be seen and they are not very well distributed. This is probably because the solution was not sonicated, and because TFA does not react with or dissolve the iron oxide. From the surface image of the FeN-film (not shown), it was not possible to see any metal particles.

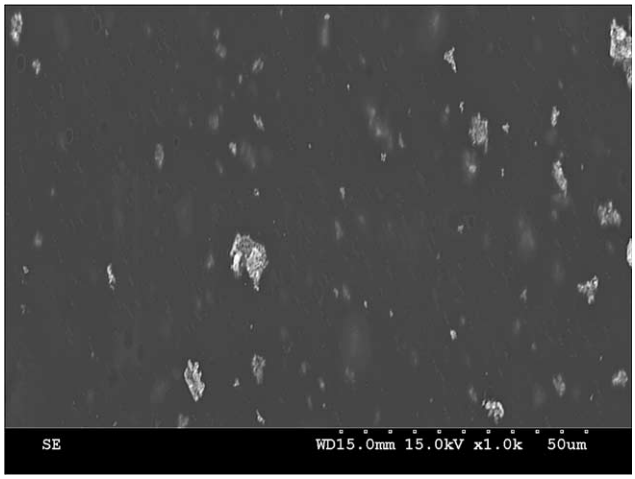

Fig. 9. SEM picture of the C–FeO membrane surface.

Element analysis results are shown in Table 3. As the membrane surface was not perfectly plane, there are some uncertainty in the element analysis. This may explain the high content of Al in the FeN–carbon. The cross-section of the membrane is not necessarily homogeneous, hence the surface composition may differ from the bulk composition. Discrepancies between measured and theoretical compositions may also arise from poor dispersion of the metals. Hydrogen could not be detected by this method.

The high surface concentration of Cu compared to the expected bulk concentration (Table 1), suggests that the Cu migrates to the surface, creating an additional resistance to mass transfer. Fluorine probably originates from the TFA solvent, attached to the metal as TFAc. The relatively high surface concentration of fluorine supports reaction (2) and the theory that Cu is concentrated at the surface. This migration of metal ions seems not to be the case for FeN, as is also reflected in a higher permeability. The FeN is probably dispersed in the bulk of the carbon. Tables 3 and 1 also show that FeO particles are not concentrated at the surface.

The traces of Mg, Al and Ca are most likely from the wood pulp. (For composition of wood, see [22].)

4. Conclusions

High performance carbon membranes can be made from (hemi)cellulosic materials. A cheap precursor and no catalyst demand during carbonization make the membrane material more economically attractive. No aging is observed in carbon from the pure cellulosic material, after gas tests for about 7 days. Hence, this type of carbon membrane may be a good starting point when aiming for a commercialization of carbon membranes.

Metal oxides can be added to increase the micropore volume of the carbon matrix (i.e. disturb the packing of graphene sheets) and promote electronic interactions with CO_2. The rationale behind an oxide additive was to utilize the surface diffusion mechanism for enhanced CO_2 transport. However, oxides (e.g. MgO) retard the transport of easily condensable gases like CO_2 and O_2.

Table 3
Surface composition [wt.%] of selected membranes as obtained from element analysis (ND = not detected)

Sample	C	O	Mg	Al	Ca	Fe or Cu	F
C	85.66	14.06	ND	0.06	0.22	ND	ND
C–FeO	82.45	14.72	0.43	0.06	0.16	2.18	ND
C–FeN	85.63	12.51	0.33	0.69	0.16	0.68	ND
C–CuN	76.39	12.48	0.76	ND	0.24	8.40	1.73

This may be exploited to improve selectivity when separating H_2 from CO_2, but is a disadvantage in biogas separation and in air separation. Due to strong adsorption in the membrane matrix the aging effect is also pronounced for oxide-containing carbons.

An undesired strong adsorption in the metal oxide–carbon membrane could be eliminated by (i) reducing the heat of adsorption (changing the type of metal), by (ii) increasing the mean pore size or by (iii) running the membrane process at a higher temperature.

Adding metal nitrates has a different effect on the separation performance. The carbon films then have a reduced methane permeability. At the same time, condensable gases are not strongly hindered, leading to an appreciable increase in both the CO_2/CH_4 and the H_2/CH_4 selectivities.

Acknowledgements

Authors want to thank research fellow David Vaaler and the Paper and Fibre Research Institute (PFI) in Trondheim for supplying cellulose materials.

We also acknowledge David Grainger in our research group for preparing and testing the $AgNO_3$-containing membrane, and for useful discussions and comments.

The interaction and correspondence with prof. WJ Koros and research fellow PJ Williams, both at Georgia Institute of Technology, Atlanta, on carbon membranes in general, is also gratefully acknowledged.

References

[1] Koresh J, Soffer A. A molecular sieve carbon membrane for continuous process gas separation. Carbon 1984;22:225.

[2] Yamamoto M, Kusakabe K, Hayashi J, Morooka S. Carbon molecular sieve membrane formed by oxidative carbonization of a copolyimide film coated on a porous support tube. J Membr Sci 1997;133:195–205.

[3] Park HB, Jung CH, Kim YK, Nam SY, Lee SY, Lee YM. Pyrolytic carbon membranes containing silica derived from poly(imide siloxane): the effect of siloxane chain length on gas transport behavior and a study on the separation of mixed gases. J Membr Sci 2004;235:87–98.

[4] Li Z, Kusakabe K, Morooka S. Preparation of thermostable amorphous Si–C–O membrane and its application to gas separation at elevated temperatures. J Membr Sci 1996;118:159–68.

[5] Barsema JN, Balster J, Jordan V, van der Vegt NFA, Wessling M. Functionalized carbon molecular sieve membranes containing Ag-nanoclusters. J Membr Sci 2003;219:47–57.

[6] Horiuchi T, Hidaka H, Fukui T, Kubo Y, Horio M, Suzuki K, Mori T. Effect of added basic metal oxides on CO_2 adsorption on alumina at elevated temperatures. Appl Catal A—Gen 1998;167:195–202.

[7] Vinke P, van der Eijk M, Verbree M, Voskamp AF, van Bekkum H. Modification of the surfaces of a gas-activated carbon and a chemically activated carbon with nitric acid, hypochlorite and ammonia. Carbon 1994;32:675–86.

[8] Soffer A, Gilron J, Saguee S, Hed-Ofek R, Cohen H. Process for the production of hollow carbon fiber membranes. European Patent 95103272.1; 1995.

[9] O'Brien KC, Koros WJ, Barbari TA, Sanders ES. A new technique for the measurement of multicomponent gas transport through polymeric films. J Membr Sci 1986;29:229–38.

[10] Coleman MR. Isomers of fluorine-containing polyimides for gas separation membranes. University of Texas, Austin, TX, USA, PhD Thesis; 1989.

[11] Breck DW. Zeolite molecular sieves: structure, chemistry and use. New York: Wiley; 1974. 636–636.

[12] Silverstein MS, Youval N, Grader GS, Shter GE. Complex formation and degradation in poly(acrylonitrile-co-vinyl acetate) containing copper nitrate. J Polym Sci Part B: Polym Phys 2004;42:1023–32.

[13] Robeson LM. Correlation of separation factor versus permeability for polymeric membranes. J Membr Sci 1991;62:165–85.

[14] Southward RE, Thompson DW, Inverse CVD. A novel synthetic approach to metallized polymeric films. Adv Mater 1999;11:1043–7.

[15] Steel K, Koros WJ. Investigation of porosity of carbon materials and related effects on gas separation properties. Carbon 2003;41:253–66.

[16] Singh-Ghosal A, Koros WJ. Air separation properties of flat sheet homogeneous pyrolytic carbon membranes. J Membr Sci 2000;174:177–88.

[17] Shao L, Chung TS, Wensley G, Goh SH, Pramoda KP. Casting solvent effects on morphologies, gas transport properties of a novel 6FDA/PMDA-TMMDA copolyimide membrane and its derived carbon membranes. J Membr Sci 2004;244:77–87.

[18] Suda H, Haraya K. Carbon molecular sieve membranes: preparation, characterization, and gas permeation properties. ACS Symposium Series, Washington DC; 2000.

[19] Tanaka K, Kita H, Okamoto K. Gas-permeability and permselectivity in polyimide films. Kobunshi Ronbunshu 1990;47:945–51.

[20] Wu J, Yuan Q. Gas permeability of a novel cellulose membrane. J Membr Sci 2002;204:185–94.

[21] Barsema JN, van der Vegt NFA, Koops GH, Wessling M. Ag-functionalized carbon molecular-sieve membranes based on polyelectrolyte/polyimide blend precursors. Adv Funct Mater 2005;15(1):69–75.

[22] Gaur S, Reed TB. An atlas of thermal data for biomass and other fuels. NREL/TP-433-7965, National Renewable Energy Laboratory, Golden, Colorado; 1995.